

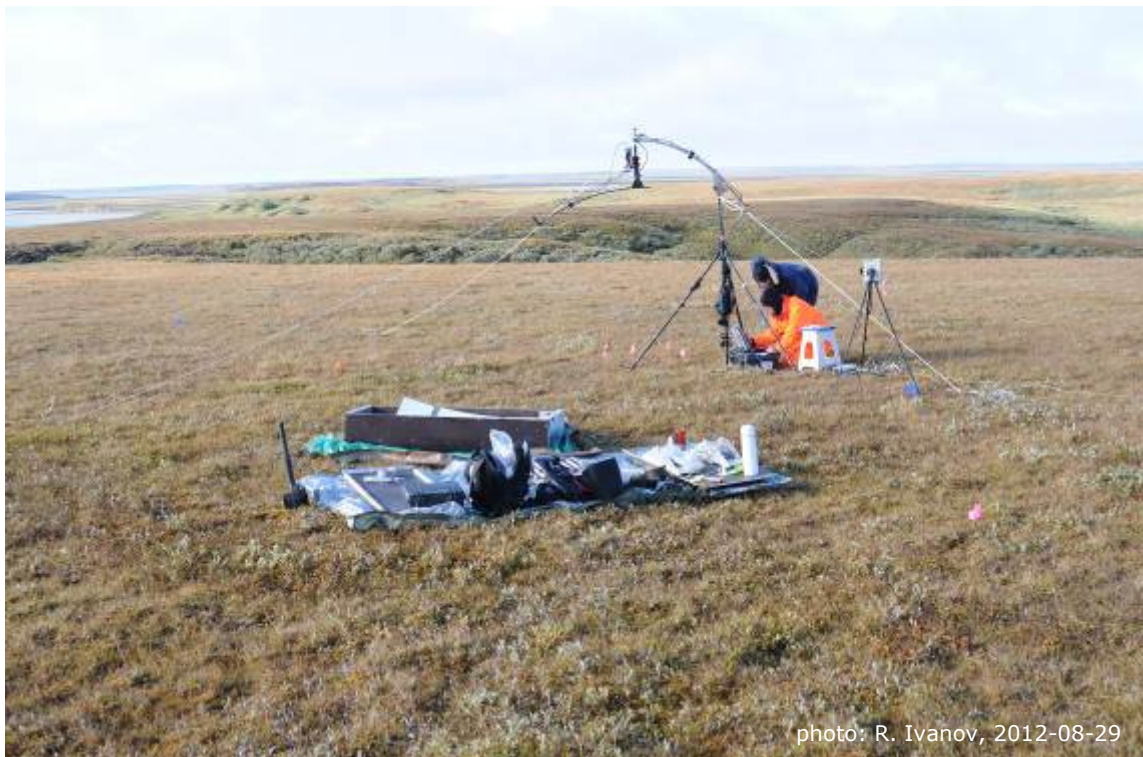


# YAMAL2011 Expedition

11<sup>th</sup> July to 9<sup>th</sup> September, 2011

## Part: AWI Data Report

25<sup>th</sup> July to 9<sup>th</sup> September, 2011



B. Heim, M. Buchhorn, H.-W. Hubberten

Alfred Wegener Institute for Polar and Marine Research (AWI)

Germany

funded by DLR/BMWi 50 EE 1013

- Gefördert von der Raumfahrt-Agentur des Deutschen Zentrums für Luft- und Raumfahrt e.V. mit Mitteln des Bundesministeriums für Wirtschaft und Technologie aufgrund eines Beschlusses des Deutschen Bundestages unter dem Förderkennzeichen 50 EE 1013 -

## List of Acronyms

ANIF	Anisotropy Factor
ASD	Analytical Spectral Devices
AVHRR	Advanced Very High Resolution Radiometer
AWI	Alfred Wegener Institute for Polar and Marine Research
BRDF	Bidirectional Reflectance Distribution Function
BRF	bidirectional reflectance factor
CALM	Circumpolar Active Layer Monitoring
ECI	Earth Cryosphere Institute
EnMAP	Environmental Mapping and Analysis Program
EyeSight	EnMAP-specific field spectro-goniometer
fAPAR	fraction of Absorbed Photosynthetically Active Radiation
FOV	Field of View
GER	Spectrometer of the company SVC (Spectra Vista Corporation)
GFZ	German Research Centre for Geosciences Potsdam
hy-Arc-VEG	hyperspectral Arctic VEGetation Indices
LAI	Leaf Area Index
LCLUC	Land Cover/Land Use Change
MERIS	Medium Resolution Imaging Spectrometer
MODIS	Moderate-Resolution Imaging Spectroradiometer
NAAT	North American Arctic Transect
NASA	National Aeronautics and Space Administration
NDVI	Normalized Differenced Vegetation Indices
NIR	Near Infrared
VI	vegetation indices
$\theta_s = \text{SZA}$	sun zenith angle
$\theta_v$	sensor zenith
$\Phi_s = \text{SAA}$	sun azimuth angle
$\Phi_v$	sensor azimuth

## Introduction

The YAMAL2011-expedition of the teams of the Earth Cryosphere Institute (ECI), Siberian Branch of the Russian Academie of Science, RU; the University Virginia, US; the University of Alaska Fairbanks, US; and the Alfred Wegener Institute for Polar and Marine Research (AWI), DE, took place as part of the NASA Yamal Land Cover/Land Use Change (NASA Yamal-LCLUC) program during the period from 11<sup>th</sup> July to 9<sup>th</sup> September 2011. Marina Leibman, chief research scientist at the ECI Moscow was the scientific and logistic expedition leader of the YAMAL2011-expedition. The field work of the AWI expedition team, Birgit Heim and Marcel Buchhorn, took place from the 1<sup>st</sup> August to 1<sup>st</sup> September 2011 in Yamal. The AWI colleagues, Kirsten Elger and Patrick Gerlach, assisted the YAMAL2011-expedition in Moscow, at the ECI (25<sup>th</sup> to 29<sup>th</sup> July; 7<sup>th</sup> to 9<sup>th</sup> September 2011).

The AWI-project 'hyperspectral Arctic VEGetation Indices' (hy-Arc-VEG) is funded by the national preparation program for the Environmental Mapping and Analysis Program, EnMAP, (German hyperspectral space mission, expected launch date in 2015) under the contract number DLR/BMWi 50 EE 1013. A major part of the project 'hy-Arc-VEG' focuses on spectro-radiometrical field measurements of a wide range of different surface types (vegetation, vegetation structure, moisture regimes) of tundra to technically explore the potential of multispectral- to hyperspectral satellite data in respect to the low-growing tundra biomes. Representative ground data need to come from well-described and well-investigated sites of a homogenous surface type. Since 2007, the NASA Yamal-LCLUC team has established such type of investigation sites in Western Siberia to sample homogenous surface types that are representative for coarse-scale remote sensing applications (e.g., at Laboravaya and Vaskiny Dachi, per site 5 transects à 50 m, 5 réleves à 5 m x 5 m).

At the Yamal2011-expedition, six of the Yamal-LCLUC investigation sites have been revisited in summer 2011: at Laboravaya, Southern Yamal, close to the Polar Ural mountains, and at Vaskiny Dachi, Northwest Yamal. At Laboravaya are two sites established, Laboravaya-1, LA1, and Laboravaya-2, LA2. At Vaskiny Dachi three sites are established, Vaskiny Dachi-1, VD1, Vaskiny Dachi-2, VD2, Vaskiny Dachi-3, VD3. M. Leibman had established the Circumpolar Active Layer Monitoring (CALM) site in the early 90s with 121 grid nodes that is revisited every year for late-summer measurements of the active layer depth. The sites represent a range of types of moss-, and lichen tundra biomes with dry to moist moisture regimes and according vegetation structure (height, above-moss biomass, species composition).

The main research goals addressed by the AWI team are:

(i) spectro-radiometrical characteristics of Tundra biomes to investigate remote sensing algorithms for spectral narrow-band and broad-band vegetation indices (VI): Normalized Differenced Vegetation Indices (NDVI), Leaf Area Index (LAI), fraction of Absorbed Photosynthetically Active Radiation (fAPAR).

(ii) anisotropy studies on spectral reflectances using an in-house (at AWI) developed field spectro-goniometer. The spectro-radiometrical multi-zenith, multi-azimuth measurements simulate the viewing geometries of wide-angle looking satellite sensors such as AVHRR, MODIS, MERIS or sensors with technical side-looking possibilities such as the EnMAP sensor (German hyperspectral space mission). The Bidirectional Reflectance Distribution Function (BRDF) characteristics of low-growing tundra biomes have not been investigated in depth so far (Vierling et al., 1997). BRDF gives the reflectance of a target as a function of illumination geometry and viewing geometry. Data on BRDF characteristics are needed for the correction of view and illumination angle effects of optical remote sensing data. A spectro-goniometer is a mechanical device for the spectro-radiometric measurement of the reflectance characteristics of a surface under a freely selectable angle of sensor azimuth,  $\Phi_v$ , and sensor zenith (viewing angle),  $\theta_v$ , and at-site given ranges of angle of sun azimuth,  $\Phi_s$ , and sun zenith,  $\theta_s$  (depending on latitude, longitude).

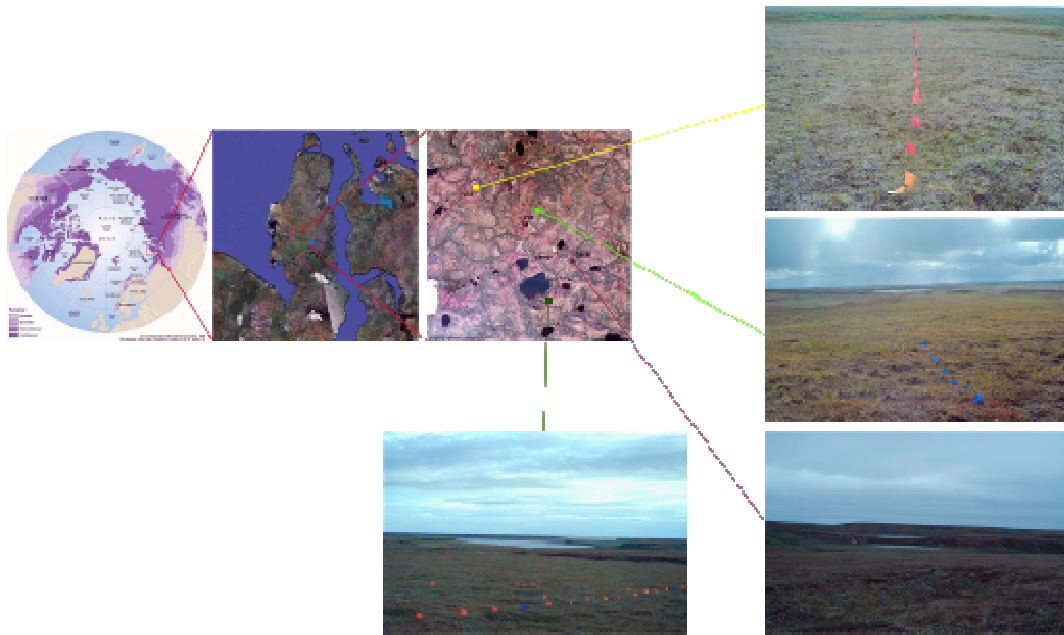


Figure 1: Vaskiny Dachi: VD1, VD2, VD3, and the Circumpolar Active Layer Monitoring (CALM) site. (photos: M. Buchhorn, AWI)

## YAMAL2011 Spectro-radiometrical Field Measurements

The established transects and réleves of the Yamal Land Cover/Land-Use Change project (Walker et al. 2008, 2009) have been re-visited and measured during the YAMAL2011-expedition (see also tables 1; 2a,b,c):

- at Laboravaya, the sites LA1 and LA2, transects (T09 to T18) and réleves (R15 to R24) (fig. 2a,b; see also Walker et al., 2008, 2009).
- at Vaskiny Dachi, the sites VD1, VD 2, and VD3, transects (T19 to T33) and réleves (R25 to R39) (fig. 3a,b,c; see also Walker et al., 2008, 2009).

Also, we had planed to carry out spectro-radiometrical measurements at the transects and réleves of the newly established Yamal-LCLUC site Kharp (July 2011) within the taiga-tundra transition zone. However, technical transportation problems limited our activities, and we kept to spectro-radiometrically measuring a range of spectral types of ‘red tundra’ near Kharp in late August (fig. 4).

The transects and réleves at LA1 and LA2, as well as at VD1, VD2, and VD3, were measured using field spectro-radiometers with sampling the nodes of the transects and within the réleves, according to Walker et al. (2008, 2009). More measurement plots (n= 123) were established along a new CALM transect, Tr11, (1.5 km long) crossing different permafrost regimes and vegetation biomes (fig. 5a,b). Moreover, new plots have been established across two landslides, Ls1, and Ls2, (fig. 6a,b). Also at VD, the CALM site with a grid of 121 points (fig. 7a,b) was re-sampled and measured.



Figure 2a. Laboravaya-1, LA1, rélevés, the old markings are still visible. (photo: M. Andreeva, ECI, 2011-08-06)



Figure 2b. Laboravaya-2, LA2, setting up the flags along the transects and rélevés. (photos: M. Buchhorn, AWI, 2011-08-06)



Figure 3a. Vaskiny Dachi-1, VD1, setting up the flags along the transects and rélevés. (photo: M. Buchhorn, AWI, 2011-08-13)



Figure 3b. Vaskiny Dachi-2, VD2, marked transects and rélevés. (photo: M. Buchhorn, AWI, 2011-08-26)

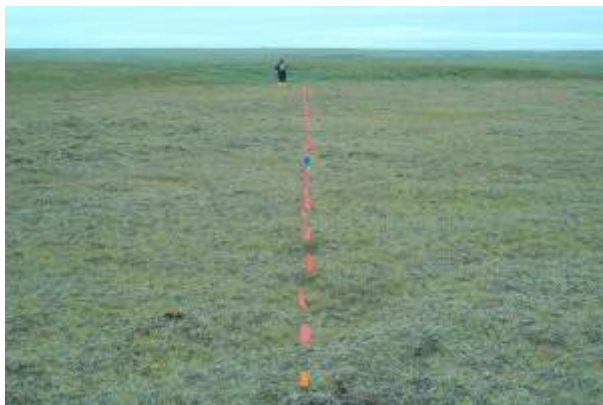


Figure 3c. Vaskiny Dachi-3, VD3, spectro-radiometrical measurements along the transects. (photo: M. Buchhorn, AWI, 2011-08-23)



Figure 4. red tundra near Kharp. (photos: M. Buchhorn, AWI, 2011-09-04)



*Figure 5a,b: new CALM transect (1.5 km long), Tr11, crossing different permafrost regimes and vegetation biomes. (photos: B. Heim, AWI, 2011-08-18).*



*Figure 6a. wetland, Northern land slide, Ls2. (photo: B. Heim, AWI, 2011-08-29).*

*Figure 6b. View from terrace down to Southern land slide, Ls1. (photo: A. Khomutov, ECI, 2011-08-20).*



*Figure 7a. CALM site, drilling of the borehole of the Thermal-State-of-Permafrost, TSP, program. The grid-nodes are marked by wooden stakes that are severely affected by slope creeping. (photo: B. Heim, AWI, 2011-08-25)*

*Figure 7b. CALM site, View down into the erosional gully where a wetland has been established. The wooden stakes of the CALM grid nodes are severely affected by slope creeping and are not upright anymore. (photo: M. Buchhorn, AWI, 2011-08-21).*

Table 1a: YAMAL2011; expedition team in the field during 1th August to 1th September, 2011

<b>Institute</b>	<b>person</b>
AWI, DE	Birgit Heim
AWI, DE	Marcel Buchhorn
Lomonossov, RU	Yuri Dvornikov
Lomonossov, RU	Alexei Gerasimov
ECI, Tyumen, RU	Maria Andreeva (named Masha)
ECI, Moscow, RU	Marina Leibman
ECI, Moscow, RU	Kseniya Ermokhina (named Ksusha)
associated	Roman Ivanov
ECI, Tyumen, RU	Evgeny Elantcev (named Genya)
ECI, Tyumen, RU	Artem Khomutov

Table 1b: YAMAL2011; field activity codes and person codes

<b>field activity codes</b>	<b>person codes</b>
00=site description	B= Birgit
01=photo VIS	M=Marcel
02=photo NIR	Y=Yuri
03=EyeSight	A=Alexei
04=ASD	Ms=Masha
05=GER	Ma=Marina
06=Munsell Colour	K=Ksusha
07=Braun Blanquet (veg/soil; functional groups, species)	R=Roman
08=Card Box	G= Genya
09=biomass	At=Artem
10=SPAD	
11=GPS coordinates	
12=Rising Plate	
13=360° panorama	
14=water sample	
15=soil sample	
16=tachymetry	

Table 2a YAMAL2011: Spectro-radiometrical measurements at Laboravaya (Yamal)

<i>site _ID</i>	<i>station name</i>	<i>_ID</i>	<i>date_code</i>	<i>equipm _ID</i>	<i>activity pers#</i>	<i>activity descr#</i>
LA	Laborovaya-2	2	20110806	1,2,4, 5,test6,13	B, M, Ms, Y, A, G, At	LA2 réleves, LA2 transects
LA	Laborovaya-2	2	20110806	4	B, B04	T14, T15, T16, T17, T18
LA	Laborovaya-2	2	20110806	5	M, M05	R20, R21, R22, R23, R24
LA	Laborovaya-1	1	20110806	1,4,5	B, M, Ms, Y, A, G, At	LA1 réleves, LA1 transects
LA	Laborovaya-1	1	20110806	4,5	B, B04, B05	T09, T10, T11, T12, T13
LA	Laborovaya-1	1	20110806	4	M, M05	R15, R16, R17, R18, R19

Table 2b YAMAL2011: Spectro-radiometrical measurements at Vaskiny Dachi (Yamal)

<i>site _ID</i>	<i>station name</i>	<i>_ID</i>	<i>date_code</i>	<i>equipm _ID</i>	<i>activity pers#</i>	<i>activity descr#</i>
VD	Vaskiny Dachi 1	1	20110812	5	B, B05	T19, T20, T21, T22, T23
VD	Vaskiny Dachi 1	1	20110812	3	M,A; M03	BRDF R28
VD	Vaskiny Dachi 1	1	20110815	1	B, B01	VD1 transects, photos
VD	Vaskiny Dachi 1	1	20110817	4	B, B04	techniquial tests: VD1 area, R25
VD	Vaskiny Dachi 1	1	20110817	5	M, M05	R25, R26, R27, R28, R29; willows
VD	Vaskiny Dachi CALM	C	20110821	13	B,M; M13	CALM grid nodes 1-121
VD	Vaskiny Dachi 1	1	20110822	4	B, B04	T19, T20, T21, T22, T23
VD	Vaskiny Dachi 3	3	20110823	4	B, B04	T29, T30, T31, T32, T33, R35, R36, R37, R38,R39
VD	Vaskiny Dachi 3	3	20110823	5	M, M05	R35, R36, R37, R38, R39
VD	Vaskiny Dachi 3	3	20110823	1	Ms, Ms01	T29, T30, T31, T32, T33, R35, R36, R37, R38,R39
VD	Vaskiny Dachi S' Landslide	Ls1	20110825	1,5	M, M01, M05	Ks01-21
VD	Vaskiny Dachi CALM	C	20110825	4	B, B04	CALM grid 1-88
VD	Vaskiny Dachi CALM	C	20110826	4	B, B04	CALM grid 89-121
VD	Vaskiny Dachi 2	2	20110826	5	M, M05	R30, R31, R32, R33, R34
VD	Vaskiny Dachi 2	2	20110828	4	Y, Y04	T24, T25, T26, T27, T28
VD	Vaskiny Dachi 2	2	20110828	1	B, B01	T24, T25, T26, T27, T28
VD	Vaskiny Dachi S' Landslide	Ls1	20110828	1,5	M, M01, M05	Ks22-24, Ks47-83
VD	Vaskiny Dachi S' Landslide	Ls1	20110828	6	R, R06	Ks01-21
VD	Vaskiny Dachi 1	1	20110829	3	M,B,R; M03, M01, M02, M06, M07, M08, M10	BRDF R25
VD	Vaskiny Dachi N' landslide Transect2011	Ls2, Tr11	20110830	5	B, B05	Ls2-01-05 Ks25-46, Ks84-95
VD	Vaskiny Dachi Transect2011	Tr11	20110830	6	R, R06	Ks25-46, Ks84-128
VD	Vaskiny Dachi Transect2011	Tr11	20110831	5	B, B05	Ks96-115

Table 2c YAMAL2011: coordinates of the investigation sites

<i>site_ID</i>	<i>station name</i>	<i>_ID</i>	<i>Lat_start</i>	<i>Long_start</i>	<i>Lat_end</i>	<i>Long_end</i>
LA	Laborovaya 1	1	N 67 42.396	E 067 59.971		
LA	Laborovaya 2	2	N 67 41.694	E 068 02.270		
VD	Vaskiny Dachi 1	1	N 70 16.538	E 068 53.469		
VD	Vaskiny Dachi 2	2	N 70 17.739	E 068 53.051		
VD	Vaskiny Dachi 3	3	N 70 18.060	E 068 50.580		
VD	Vaskiny Dachi CALM	C	N 70 17.051	E 068 54.411		
VD	Vaskiny Dachi S' Landslide	Ls1	N 70 17.085	E 068 53.950		
VD	Vaskiny Dachi N' landslide	Ls2	N 70 17.620	E 068 55.551		
VD	Vaskiny Dachi Transect2011	Tr11	N 70 17.076	E 068 54.695	N 70 17.707	E 068 55.566
KA	Site near Kharp	KA	N 66 45.578	E 065 58.013		

We used a portable FieldSpec® Pro spectro-radiometer (350-2400nm) (AnalyticalSpectral Devices, Boulder, CO) and two GER® 1500 field spectrometers (350-1050nm) provided by the GFZ (German Research Centre for Geosciences). For the standard measurements, both spectrometer types, ASD and GER, were equipped with a 8° Field-Of-View (FOV) fore-optic for the radiance measurements. Also, experimental measurements using a 4° FOV fore-optic for the GER and a 25° FOV fore-optic for the ASD were carried out. For irradiance measurements, the spectrometers are equipped with a cosine diffuser optic.

The in-house (at AWI) developed EnMAP-specific field spectro-goniometer, named EyeSight, was patented in 2011 and the current set-up is equipped with the two GER1500 spectro-radiometers (fig. 8a,b,c). The spectrometer installed on the EyeSight spectro-goniometer measures the upwelling radiance [ $\text{W m}^{-2} \text{sr}^{-1} \text{nm}^{-1}$ ] of the surface (target). The optic of the spectrometer can be moved in circles around all the azimuth angles, and can be installed along the arc up to 30° sensor viewing angle. The reference measurements of a white reference Spectralon© plate is frequently made at the start and the end of each measurement cycle. In parallel, the second spectrometer installed on a tripod, continuously measures the downwelling irradiance [ $\text{W m}^{-2} \text{nm}^{-1}$ ] using a cosine diffuser installed on a 8° FOV fore-optic.

The BRDF measurements can only be carried out during optimal sky conditions. Due to the severe weather limitations in August 2011 (continuous storms and rains), only two rélevés of the VD1 site, RV25, and RV28, (description in Walker et al., 2009), could be measured using AWI-EyeSight. However, these plots could be measured under several sun zenith ranges.

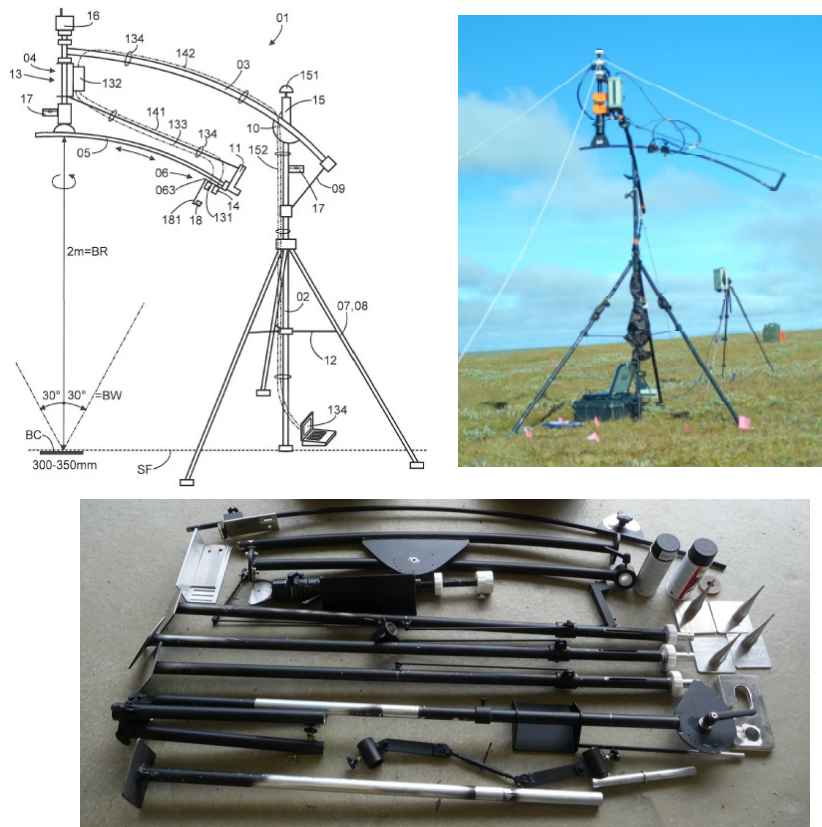


Figure 8a,b,c: EnMAP-specific field spectro-goniometer (EyeSight) a) technical graph of EyeSight; b) field set-up of EyeSight, measurements at Vaskiny Dachi, 2011-08-29; c) EyeSight disassembled into its components ready for transport. (photos: M. Buchhorn, AWI)

The calculated parameters from the field spectrometer measurements (transects, rélevés) are

- the spectral surface reflectance coefficient  $R(\lambda)$  from 400 nm to 900 nm (due to moisture-related noise the wavelengths  $> 900$  nm were removed)
- sensor-specific Normalized Differenced Vegetation Indices (NDVI):  
*multi-spectrally based indices* (broad-band indices): NDVI AVHRR, NDVI MODIS (multi-spectral land mode), NDVI Landsat, NDVI SPOT, NDVI GEOEye, NDVI QuickBird;  
*super-spectrally based indices* (high-spectral resolution band indices): NDVI MODIS (super-spectral water mode), NDVI MERIS;  
*hyper-spectrally based indices* (hyper-spectral resolution band indices): NDVI EnMAP, NDVI CHRIS/PROBA, NDVI Hyperion, NDVI field spectro-radiometry (single wavelengths-based with 1.5 nm spectral resolution);

comments: At this state, the conversion from spectro-radiometrical field measurements into the sensor-specific bands is preliminary calculated with Gaussian-fitted sensor response curves using the ENVI® software. However, this showed up to may be not adequate for the super-spectral and the multi-spectral broad-band sensors. Therefore, specific calculations involving the high-spectral resolution sensor-specific response curves still needs to be carried out.

- Fraction of Absorbed Photosynthetically Active Radiation (fAPAR) for different Tundra biomes as well as algorithms for Leaf-Area-Index (LAI) derivatives from fAPAR
- Bidirectional Reflectance Factor (BRF) in order to analyse the Bidirectional Reflectance Distribution Function (BRDF) of different Tundra biomes

Used equations:

The spectral reflectance factor,  $R(\lambda)$ , is calculated as

$$R(\lambda) = \frac{L_{up}(\lambda)}{L_{in}(\lambda)} \quad (1)$$

$R$ = reflectance [dimensionless]; x 100 [%]

$L_{in}$ = incoming (downwelling) radiance [ $\text{W m}^{-2} \text{sr}^{-1} \text{nm}^{-1}$ ] (measured back-reflected from the Spectralon© reference plate)

$L_{up}$ = upwelling radiance [ $\text{W m}^{-2} \text{sr}^{-1} \text{nm}^{-1}$ ] (measured back-reflected from the surface/target)

The Normalized Differenced Vegetation Indices, NDVI, is calculated as

$$NDVI = \frac{R_{NIR} - R_{red}}{R_{NIR} + R_{red}} \quad (2)$$

NDVI= Normalized Differenced Vegetation Indices

$R_{NIR}$ = reflectance within the Near InfraRed, NIR, wavelength band

$R_{red}$ = reflectance within the red wavelength band

The used wavelengths for the NDVI calculation of the AVHRR, MODIS and EnMAP sensors are:

	MODIS	AVHRR	EnMAP
RED	620-670nm	580-680nm	672nm
NIR	841-876nm	725-1000nm	840nm

In case of 100% vegetation coverage, the fraction of Absorbed Photosynthetically Active Radiation,  $fAPAR$ , can be calculated as

$$fAPAR = \frac{\sum_{\lambda=400nm}^{700nm} [\pi \cdot L_{in}] - \sum_{\lambda=400nm}^{700nm} [\pi \cdot L_{up}]}{\sum_{\lambda=400nm}^{700nm} [\pi \cdot L_{in}]} \quad (3)$$

$fAPAR$ = fraction of Absorbed Photosynthetically Active Radiation

$L_{in}$ = incoming (downwelling) radiance [ $\text{W m}^{-2} \text{sr}^{-1} \text{nm}^{-1}$ ] (measured back-reflected from the Spectralon© reference plate) **or** measured directly as incoming (downwelling) irradiance,  $E_{in}$ , [ $\text{W m}^{-2} \text{nm}^{-1}$ ] with the cosine diffuser, then use  $\sum_{\lambda=400nm}^{700nm} E_{in}$  instead of  $\sum_{\lambda=400nm}^{700nm} (\pi \cdot L_{in})$

$L_{up}$ = upwelling radiance [ $\text{W m}^{-2} \text{sr}^{-1} \text{nm}^{-1}$ ] (measured back-reflected from the surface/target)

The Bidirectional Reflectance Factor, BRF, is calculated

$$BRF(\lambda, \theta_s, \phi_s, \theta_v, \phi_v) = \frac{[L_{up}(\lambda, \theta_s, \phi_s, \theta_v, \phi_v)(t_2)](t_1)}{L_{in}(\lambda, \theta_s, \phi_s)(t_1)} \cdot R_{REF} \quad (4)$$

BRF= Bidirectional Reflectance Factor

$L_{in}$ = incoming (downwelling) radiance [ $\text{W m}^{-2} \text{sr}^{-1} \text{nm}^{-1}$ ] (measured back-reflected from the Spectralon© reference plate)

$L_{up}$ = upwelling radiance [ $\text{W m}^{-2} \text{sr}^{-1} \text{nm}^{-1}$ ] (measured back-reflected from the surface/target)

$R_{REF}$ = Reflectance function of the Spectralon reference plate

[...](t) = stands for linear interpolation of bracket contents to time t

$\theta_s$  = sun zenith;  $\Phi_s$  = sun azimuth;  $\theta_v$  = sensor zenith;  $\Phi_v$  = sensor azimuth;

The time interpolation [...] (t) is needed in order to bring all measurements to the time of the upwelling measurement by using the irradiance measurement of a second spectrometer measurement.

$$L(x) = L(t) \cdot \frac{E(x)}{E(t)} \quad (5)$$

L = radiance [W m<sup>-2</sup> sr<sup>-1</sup> nm<sup>-1</sup>]

E = irradiance [W m<sup>-2</sup> nm<sup>-1</sup>]

(x) = searched time stamp

(t) = given time stamp

## Discussion of first results

(i) The reflectance spectra types of the Laboravay, LA1, LA2, and Vaskiny Dachi, VD1, VD2 and VD3 surfaces show low reflectance peaks in the green wavelength range, low absorption depths in the red wavelength band and smooth Near InfraRed, NIR, reflectance shoulders (e.g., fig. 9 and fig. 12). This observation confirms a reflectance type that is caused by the low multiple scattering activities in the NIR that is typical for a low-growing vegetation structure. The green reflectance peak seems to be degraded due to absorption by carotinoides and anthocanides in the greenish-to red wavelength range. The greenish-to short red wavelength range has no effect on the NDVI or similar VI constructed using the broad red and the NIR wavelength range. However, tundra-specific reflectance types result always in a range of low NDVI values due to low scattering activities in the NIR. Currently, the data sets are processed to evaluate the ranges and statistical parameters.

(ii) The first results of the BRDF analyses do not show the theoretical behaviour of BRDF from homogeneous vegetated surfaces. The theoretical shape of a BRDF is that the minimum reflectance usually displaced towards the forward scattering direction and the maximum reflectance in the backward direction.

The first BRDF calculations for the tundra réleve plots VD1 R25 and VD1 R28 with 10 to 15 % vascular plant cover on 100% moss cover proof the mirror asymmetry in relative azimuth with respect to the principal plane. The BRDF calculations also show the maximum scattering displaced in the backward direction, but no minimal forward scattering. Instead, the forward scattering from the moss-dominated tundra type is characterised by similar to higher reflectance values in the forward scattering direction (see figures 9, 10, 11).

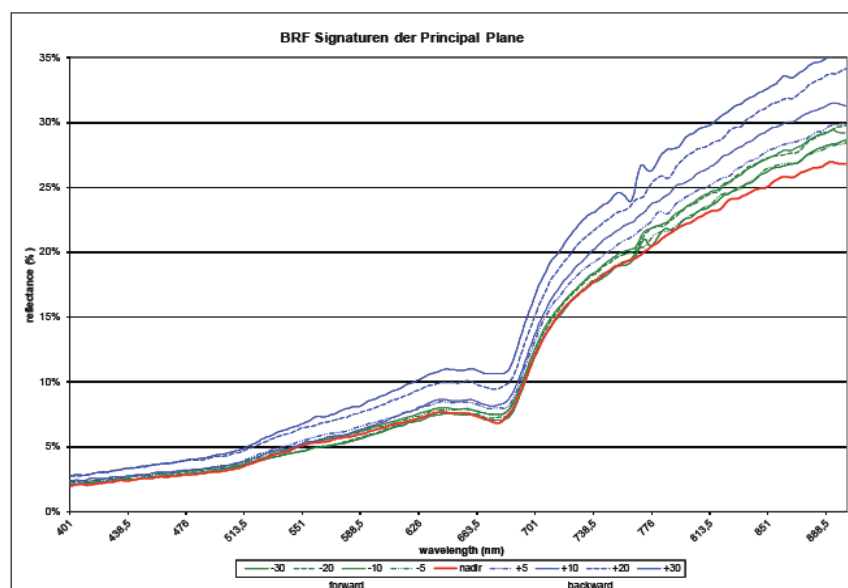


Figure 9: forward and backward reflectance measured at VD1, réleve25, R25 (2012-08-29).

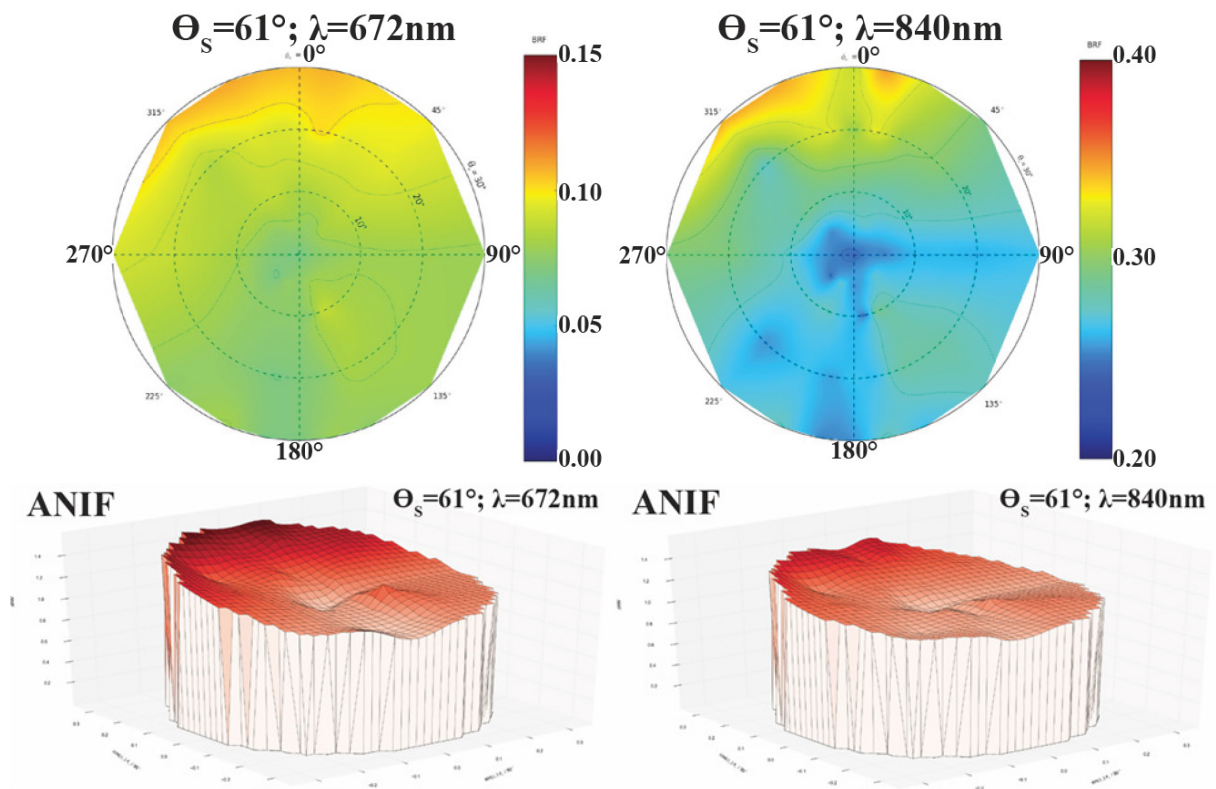


Figure 10: ANISotropy Factors, ANIF, of the red wavelength (675 nm) and the NIR wavelength (840 nm) at plot VD1, réleve25, R25 (2012-08-29). Sun Zenith Angle, SZA,  $\theta_s = 61^\circ$ .

The ANISotropy Factor, ANIF, is normalized to the nadir value. The 2-dimensional and 3-dimensional BRDF ANIF graphs of the red wavelength (672nm) and the NIR Wavelength (840nm) visualize this BRDF effect (figure 10). Highest influence is viewable in the backward direction.

The red and the NIR wavelength bands are used to calculate the NDVI (equation 2). The 2-dimensional BRDF NDVI graphs (AVHRR NDVI, MODIS NDVI, EnMAP NDVI) show that the BRDF effect is also visible for the NDVI (figure 11). The Gaussian-fitted response curves of the AVHRR, MODIS and EnMAP sensors were used to calculate the reflectance within the sensor spectral bands.

The band width and center position of the RED- and NIR-sensor bands that are the input bands into the NDVI calculation has only an influence on the absolute NDVI values, but the BRDF effect appears in all with the same intensity.

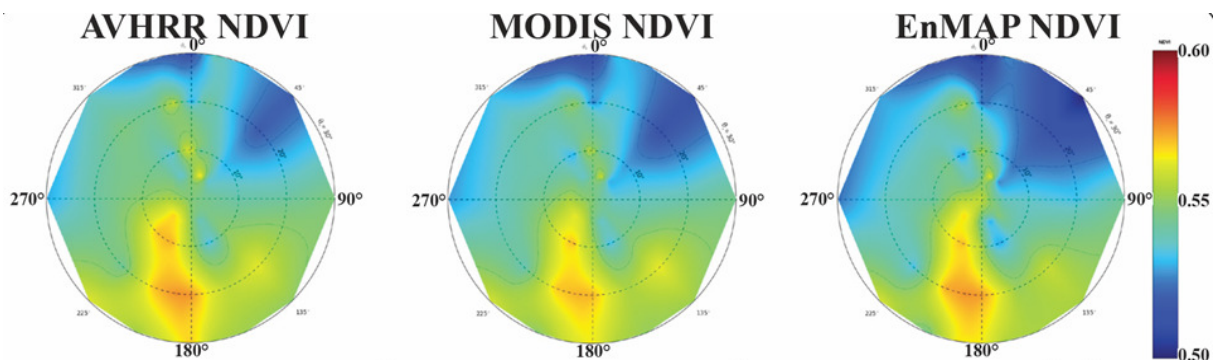
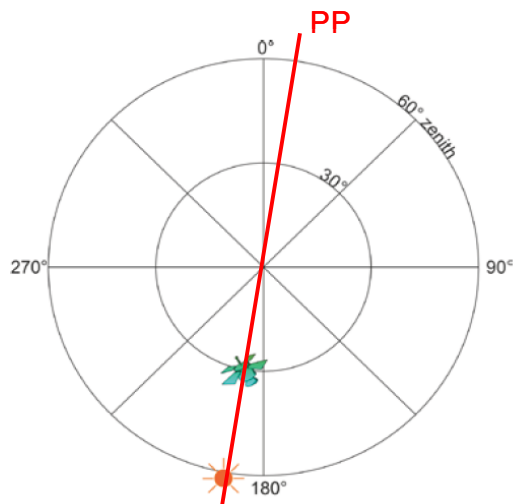
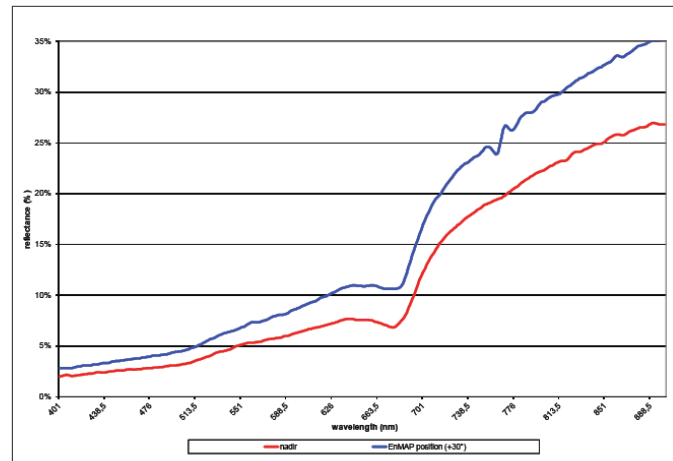


Figure 11: NDVI comparison (AVHRR, MODIS, EnMAP) at plot VD1, réleve25, R25 (2012-08-29).



Messung VD1\_RV25\_03  
 SZA: 61°  
 SAA: 190°



Vegetation: dwarf-shrub-moss tundra

Figure 12: sun-target-satellite position with the highest BRDF effect on the Tundra vegetation at plot VD1, réleve25, R25 (2012-08-29): Sun Zenith Angle (SZA) = 61°; Sun Azimuth Angle (SAA) = 190°; PP=Principal Plane. The graph of reflectance curves shows the nadir measurement (red line) and the highest BRDF effect in the backward-looking geometry at 30° sensor-viewing angle (blue line) with SZA = 61°; SAA = 190°.

The sun-target-EnMAP constellation for the réleve25, R25, at a Sun Zenith Angle (SZA) of 61° and a satellite position of 30° in backward direction (sun-satellite-target line) shows the highest BRDF influence on the spectral signature of the low-growing tundra (figure 12). The reflectance of the 30° backward position (blue line, figure 12) shows higher reflectance values than the reflectance of the nadir position (red line, figure 12). The spectral reflectances of the other possible sun-target-EnMAP constellations are in between the nadir and the 30° backward measurement (e.g., see also figure 9).

The analysis show that the BRDF influence on VI's of low-growing arctic biomes has to be taken into account for the development of tundra-adapted VI's. The low sun zenith angles in the Arctic latitudes prevent hotspot-effects if the sensor viewing geometry is limited by the 30° sensor viewing angle and does not tilt further, but a BRDF normalization is still needed.

More field spectro-radiometrical measurements and BRDF measurements of study sites are planned for summer 2012 along the North American Arctic Transect (NAAT) in cooperation with the University of Fairbanks Alaska, Alaska Geobotany Center.

## References

- Vierling et. al. (1997): Differences in arctic tundra vegetation type and phenology as seen using bidirectional radiometry in the early growing season. In: Remote Sensing of Environment, Jg. 60, H. 1, S. 71–82. doi.org/10.1016/S0034-4257(96)00139-3.
- Walker et al. (2008): Data Report of the 2007 Expedition to Nadym, Laborovaya and Vaskiny Dachi, Yamal Peninsula Region, Russia. Alaska Geobotany Center, Institute of Arctic Biology, University of Alaska Fairbanks, Fairbanks, AK.
- Walker et al. (2009): Data Report of the 2007 and 2008 Yamal Expeditions. Alaska Geobotany Center, Institute of Arctic Biology, University of Alaska Fairbanks, Fairbanks, AK. 121 pp.